ARTICLE INFO
Article ID: 12-01-02-0005

doi:10.4271/12-01-02-0005

Toward Improving Vehicle Fuel Economy with ADAS

Jordan Tunnell, Zachary D. Asher, Sudeep Pasricha, and Thomas H. Bradley, *Colorado State University, USA*

Abstract

Modern vehicles have incorporated numerous safety-focused advanced driver-assistance systems (ADAS) in the last decade including smart cruise control and object avoidance. In this article, we aim to go beyond using ADAS for safety and propose to use ADAS technology to enable predictive optimal energy management and improve vehicle fuel economy (FE). We combine ADAS sensor data with a previously developed prediction model, dynamic programming (DP) optimal energy management control, and a validated model of a 2010 Toyota Prius to explore FE. First, a unique ADAS detection scope is defined based on optimal vehicle control prediction aspects demonstrated to be relevant from the literature. Next, during real-world city and highway drive cycles in Denver, Colorado, a camera is used to record video footage of the vehicle environment and define ADAS detection ground truth. Then, various ADAS algorithms are combined, modified, and compared to the ground truth results. Lastly, the impact of four vehicle control strategies on FE is evaluated: (1) the existing vehicle control, (2) actual ADAS detection for prediction and optimal energy management (we consider two variants ADAS1 and ADAS2 for this strategy), (3) ground truth ADAS detection for prediction and optimal energy management, and (4) 100% accurate prediction and optimal energy management. Results show that the defined ADAS scope and algorithms provide close correlation with ADAS ground truth and can enable FE improvements as part of a prediction-based optimal energy management strategy (EMS). Our proposed approach can leverage existing ADAS technology in modern vehicles to realize prediction-based optimal energy management, thus obtaining FE improvements with minor modifications.

History

Received: 30 May 2018
Revised: 05 Sep 2018
Accepted: 15 Sep 2018
e-Available: 29 Oct 2018

Keywords

Advanced driver-assistance system (ADAS), Fuel economy (FE), Energy management strategy (EMS), Hybrid electric vehicle (HEV)

Citation

Tunnell, J., Asher, Z., Pasricha, S., and Bradley, T., "Toward Improving Vehicle Fuel Economy with ADAS," *SAE Int. J. of CAV* 1(2):2018, doi:10.4271/12-01-02-0005.

ISSN: 2574-0741
e-ISSN: 2574-075X

Introduction

Fuel economy (FE) is a significant contributor to energy consumption, where an increase in FE would significantly decrease our energy footprint [1]. This reduction would lower greenhouse gas emissions and air pollution. One leading method to increase FE is vehicle electrification [2], where hybrid electric vehicles (HEV) have helped bridge the gap between electric vehicles (EV) and combustion engines. For HEV, many control strategies have been researched and implemented to increase FE, for example, by combining the usage of the combustion engine and the electric motor [3, 4, 5]. A significant FE improvement is possible with a control strategy that utilizes the fact that electric motors are significantly more efficient than combustion engines at slower speeds.

FE improvement can occur for a fixed route through driver feedback to promote efficient habits (known as eco-driving [6]) and there is emerging research into integrating ADAS and eco-driving [7]. Conversely, for fixed speeds, the powertrain efficiency can be improved by optimizing the use of engine power and battery power [8], which is known as an Optimal Energy Management Strategy (Optimal EMS). The Optimal EMS is derived by applying the principles of optimal control to a fixed drive cycle, that is, the engine power is controlled to provide the minimal fuel consumption. For a known Optimal EMS, recent research demonstrated real-world results by including various aspects of physical vehicles [9, 10, 11, 12, 13, 14]. Note that research has also begun to show that the largest FE improvements are possible when eco-driving and an Optimal EMS are combined [15]. But, typically these FE improvement strategies require significant prediction of future events in the drive cycle, which is not straightforward. This work is novel in that we focus on the practical aspects of prediction to inform an Optimal EMS derivation.

Another aspect that is receiving growing attention in emerging vehicles is safety. The World Health Organization (WHO) has indicated that 1.25 million deaths occur from traffic accidents [16], with global costs of up to U.S. $528 billion yearly [17]. These staggering numbers have become an incentive to increase the focus on safety for automotive systems. Active safety systems have become a significant area of growth. Research in such systems has led to advances in testing [18, 19] improvement in algorithms [20, 21] and added functionality [22]. Popular active safety deployments in vehicles include adaptive cruise control, lane detection, and automatic parking. The advanced driver-assistance systems (ADAS) used for active safety require many different types of sensors such as light detection and ranging (LIDAR), radio detection and ranging (RADAR), ultrasonic sensors, and various types of imaging cameras. Figure 1 summarizes the function and location of many of these sensors. ADAS is a highly researched area in which many topics attempt to reduce cost, increase accuracy, and maintain strict safety standards. [23] is an example of an improvement seen in the ADAS field.

The use of computer vision to identify the surrounding environment and the classification of objects in a video is a significant area of research in ADAS. The use of a camera is one of the easier methods to determine the type of object that the vehicle is approaching. The general flow for this object detection includes image acquisition, pre-processing, segmentation, object detection and tracking, depth estimation, and system control. Details of how each layer works can be found in [24]. To more reliably accomplish the task of object detection, recent approaches are exploring deep learning algorithms such as convolutional neural networks (CNN) for greater accuracy.

FIGURE 1 State-of-the-art ADAS and different sensors [24].

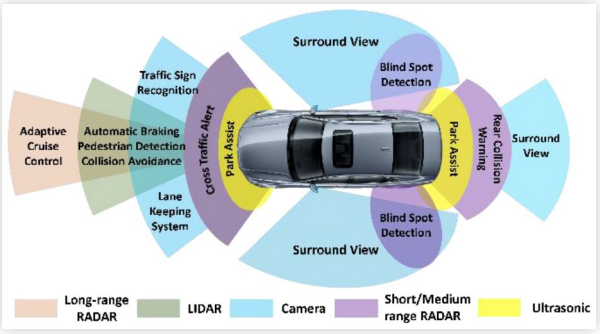

The information that ADAS requires to make decisions for safe driving can be repurposed to provide predictions for improved FE through eco-driving, an Optimal EMS, or a combination of both. Eco-driving uses ADAS in many current vehicles to implement applications such adaptive cruise control. However, an Optimal EMS requires prediction of the entire drive cycle to be globally optimal [16, 17]. Despite this seemingly difficult requirement, our initial research shows that FE improvements using limited prediction with an Optimal EMS are possible [25, 26].

In this article, we propose the use of ADAS information to generate prediction data for use in an Optimal EMS. The ADAS-generated prediction data is used to derive an Optimal EMS which is implemented in a vehicle model to improve FE. The incorporation of ADAS for prediction is novel and has not been explored in prior work [27]. Several ADAS prediction models are developed and discussed in this article, with various computer vision techniques. The approach for obtaining ADAS information for Optimal EMS is presented in detail. Our work in this article represents a promising solution to bridge the gap between vehicle electrification and autonomous systems, for the purpose of fuel efficiency improvements.

Methods

In this section, we will show how we defined the fixed drive cycle for our Optimal EMS, methods we used to acquire our ADAS information, and how we used ADAS information for our predictions.

Drive Cycle Development

Two routes for our drive cycles were defined, where the aim was to test different but equally challenging road conditions

FIGURE 2 The highway-focused drive cycle that passes through two interstates in Denver, CO, USA. Source: Google Maps.

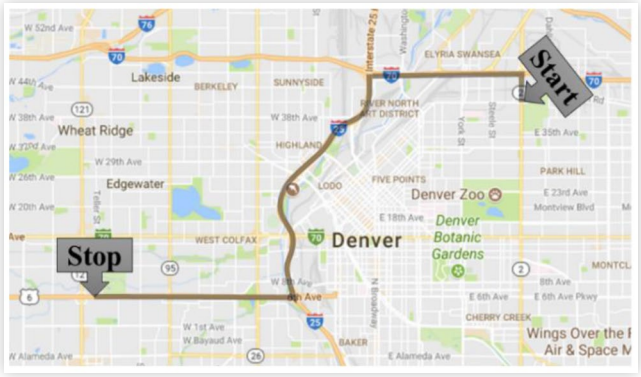

FIGURE 4 ZED stereo vision camera from stereolabs used for video capture.

in Denver, Colorado. Figure 2 shows the highway drive cycle, and Figure 3 shows the city drive cycle. Each drive cycle was driven four times alternating after each run, where run 1 was the highway cycle and run 8 was the Denver downtown (city) cycle. Alternating between routes was implemented to increase the chances of capturing different driving conditions faced on the road for each type of drive cycle.

Another motivation for these specific cycles was the relative challenge for ADAS to detect and interpret the surrounding environment around the vehicle. The chosen fixed routes contained several stop signs, many traffic lights, busy streets and highway traffic, reflective buildings, road construction, pedestrian crossings, and changing lighting conditions. Many of these cases can prove to be quite tricky for computer vision systems to analyze the environment accurately.

Data Acquisition

Several sensors were used in a test vehicle to determine vehicle speed, acceleration, and video feed of the driving environment. The vehicle information was captured from a data acquisition (DAC) device connected to the controller area network (CAN) bus. Captured data from the CAN bus included position data from the global positioning system (GPS) and vehicle speed and acceleration.

A ZED stereo vision camera [28] was used to obtain the video data needed for post-processing. In each drive cycle, the two frames of 1280 × 720 from the two (stereo) camera sensors were captured at 30 frames per second (fps) and written into a .mp4 video file. An ASUS laptop with an Intel i7 and a GeForce GTX 1070 was used both for the capture and processing of the data. As seen in Figure 4, the ZED camera was attached to a suction cup using a 3D printed mount. The optimal placement for the camera was determined to be at the top portion of the windshield of the test vehicle near the rearview mirror. This placement was based on minimizing the effect of glare and maximizing lane line, sign, and vehicle visibility. A downward camera angle could be achieved by placing the camera on the highest point of the windshield. We found that this angle reduced the effect of lighting conditions because the lens wasn't overexposed from the sun and still had a full view of the vehicle environment.

FIGURE 3 The city-focused drive cycle that passes through downtown in Denver, CO, USA. Source: Google Maps.

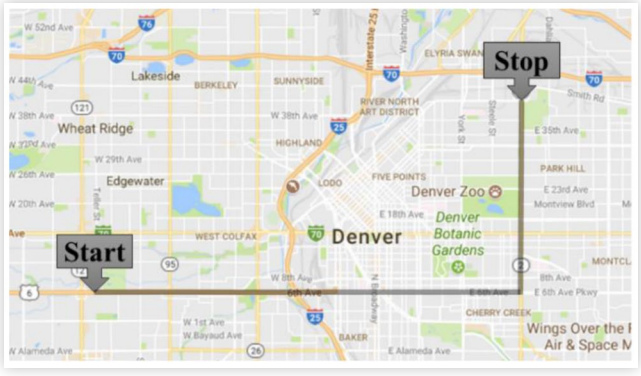

ADAS Information for Optimal EMS

Traditional ADAS track and utilize data that would allow a vehicle to drive safer. Such data includes details of vehicle location, distance of objects to the driver, lane detection, etc. However, for Optimal EMS prediction, we have determined that only the data that would directly affect vehicle speed is pertinent, that is, only this data can increase FE, when using a prediction-based global Optimal EMS. As an example if we know that the vehicle/driver is going to slow down for a while, then the Optimal EMS may elect to turn off the engine to reduce fuel consumption. Therefore, tracking the lane in which the vehicle resides is not a direct factor to the change in vehicle speed and is not necessarily a high priority. Table 1 lists the useful prediction data features for our purposes of Optimal EMS.

The data features can help identify situations where a vehicle may need to slow down. *Traffic light state* and *stop sign*

TABLE 1 Prediction data features for Optimal EMS.

ADAS EMS prediction data features	Possible output states
Time	(s)
Frame captured time	(date-time object)
Traffic light state	(r|y|g|N/A)
Stop sign state	(far|medium|close|N/A)
Vehicle in-front state	(inc|dec|same|N/A)
Turning	((in turn lane)|turning|N/A)
Speed limit	(25|30|35|40|45|55|65|75|N/A)
Stop sign ahead	(Y|N/A)
Output HZ	1

state were chosen to be features that were important to detect because of their role in regulating speed. For traffic lights, red, yellow, green, and N/A (not available) are states that were deemed to be relevant prediction data for an Optimal EMS. Stop signs define an upcoming event that would slow down the vehicle based on its relational distance. The states far (>50 m), medium (50 m < stop_sign_location < 10 m), close (<10 m), and N/A provide the prediction system with information on how quickly the system needs to brake. A situation of detecting a stop sign nearby when turning onto a street is different from finding a stop sign down the street, thus requiring a distance calculation with each stop sign.

Initially, the consideration was to detect all visible vehicles. In most cases however, we found that the only vehicle that affects the driver's speed is the one directly in the lane ahead. This simpler requirement is unlike many ADAS where almost all vehicles are tracked for safety reasons by analyzing the entire driving environment. In situations where a car in an adjacent lane merges nearby, the driver will now be in the main lane and tracked. Monitoring the driver before then would not lead to any more indication of similar situations, and therefore only the current lane needs to be tracked for vehicle activity, for our purposes. Much like the reasons stated for stop signs, we consider the scenario where the vehicle's spatial relationship to the vehicles ahead of it changes. The output states for the *vehicle in-front state* data are defined as increasing, decreasing, and same regarding distance and N/A for no vehicles in the current lane. Brake light information was considered to be redundant data and therefore left out of the tracked ADAS prediction features.

An upcoming turn often indicates a decrease in speed for a driver. Significant bends in the road or turning 90° warrants a reduction of speed, making the *turning* feature a necessary one for Optimal EMS prediction. The *speed limit* and *stop sign ahead* features indicate a change in speed and were found to also be useful for Optimal EMS prediction. The possible outputs for speed signs were the listed limit value seen in Table 1 and a yes for positive instances and N/A for no signs was used for each stop sign occurrence.

Lastly, the frequency (*output Hz*) of the information was deemed to require a 1 Hz tick rate. A 30 fps video requires an output log entry every 30 frames. Based on [25, 26], this output rate would be sufficient for prediction data for an Optimal EMS. The running time of seconds and the *frame captured time* were also needed so that the prediction system allowed for syncing other data sets such as vehicle speed.

Ground Truth Development

The data required from an ADAS system as defined in the previous section needed as close to perfect predictions as possible, to validate the need for the information. This near-perfect data is called ground truth data and is obtained by having a human closely analyze the environment instead of a computer algorithm. In this case, ground truth data at any point during a drive cycle can be referred to as a human's interpretation of the scene at that point. Each prediction data feature discussed earlier requires human-annotated data for all eight videos at a data rate of 1 Hz to obtain ground truth data. We collect this ground truth data as it can show how an Optimal EMS prediction would fare with completely accurate ADAS data.

To obtain the ground truth data, a graphical user interface (GUI) app was developed to get the values for data features defined in Table 1. A screenshot of this app can be seen in Figure 5 that also shows what each group of buttons represents. The app allowed us to watch each of the eight drive cycle videos via the GUI, pause the video at any time, and annotate/capture data by pressing the appropriate state buttons for each prediction field. After the ground truth was specified for each drive cycle video, a comma-separated value (CSV) file was generated that saved the prediction data needed for the Optimal EMS.

The vehicle in-front state was later redefined only to use the states decrease, same, and N/A. The increasing state was a difficult one to define since at far distances, determining if a vehicle remained at the same position or deviated was not easy. The experiments were rerun to use the same state for all situations when the vehicle was moving away from the driver. All other states were kept the same as defined earlier.

ADAS Detection Development

In this section, we discuss a combination of custom and known algorithms, called ADAS1 and ADAS2, that were used to automatically capture the ADAS EMS prediction features defined in Table 1. In this section, we only consider ADAS

FIGURE 5 Ground truth development app.

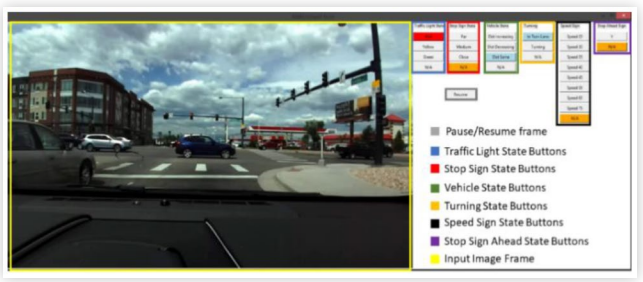

TABLE 2 Features of ADAS1 and ADAS2.

Features	Ground truth	ADAS1	ADAS2
Stop sign detection	✓	✓	✓
Vehicle detection	✓	✓	✓
Pedestrian detection	X	✓	✓
Traffic light state	✓	✓	✓
Brake light state	X	X	✓
Turning lane	✓	X	X
Speed limit	✓	X	X
Image filtering	N/A	X	✓

information that we could obtain from a stereo vision camera. Although other information from sensors discussed in the introduction section could provide useful information, it was deemed to be out of this experiment's scope.

Using the programming language Python and open-source computer vision libraries (e.g., OpenCV), we developed the ADAS1 and ADAS2 strategies to obtain the data for EMS prediction. ADAS1 and ADAS2 included the same features defined for optimal ADAS EMS prediction and a few additional fields, all of which can be seen in Table 2. After watching each video for the ground truth selection, it was determined that ADAS1 and ADAS2 did not need the ability to track the speed limit or turn state. Speed limit detection was discovered to have a low impact on the change in speed of the vehicle during developing ground truth data and therefore was omitted. In these drive cycles, the speed signs encountered did not enforce a significant reduction of vehicle speed (e.g., from 70 mph to 40 mph) that would warrant any major change in velocity. The turn state was also not included because of the difficulty of determining a turning state with computer vision. The state of the turn signal of the car as well as accelerometers provides a better indication of a vehicle changing lanes and turning. Signs indicating that there was a stop sign ahead were also not present in any of the drive cycle information, and therefore the inclusion of this detection would not lead to better prediction results and was left out of ADAS1 and ADAS2.

We considered two new features for our two ADAS strategies in addition to our ground truth set of data features: pedestrian tracking and brake light tracking. Pedestrian detection was deemed useful in the cases, though infrequent, where pedestrians would jaywalk through the road and no vehicle was in front. Most ADAS object detection algorithms support pedestrian detection, and we considered it as well to explore the effect of false positives (detecting an object that does not exist in the image) for Optimal EMS predictions. In our drive cycles, pedestrians did not lead to vehicle speed changes; hence this feature was not considered in our ground truth feature set in Table 1. Lastly, ADAS2 utilized a brake light state for situations where the vehicle distance was not changing, for example, when both vehicles are stopped at a light. For ground truth development, the idea of brake light detection was found to be redundant information because the vehicle speed was already tracked in the vehicle state. Hence this feature was not included in our ground truth feature set. But we included this feature in ADAS2 for the same reason as that for considering pedestrian tracking: to capture the effect of mispredictions due to false positives with the ADAS algorithms, during Optimal EMS prediction.

FIGURE 6 ADAS prediction pipeline.

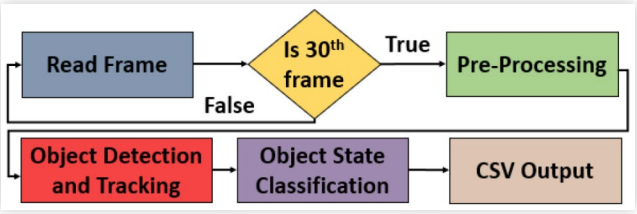

The flowchart in Figure 6 shows an overview of the ADAS prediction pipeline that we developed for both ADAS1 and ADAS2. The eight drive cycle videos were analyzed by the computer vision algorithms to generate the EMS prediction data. As discussed in an earlier section, reading every 30th frame (for a 30 fps video capture rate) for output was a simplification we used, to reduce the need for extensive computation overhead. Various pre-processing steps were applied to the frame image before sending to the object detection and tracking algorithms. Once the objects were found, the state of each ADAS EMS data feature was determined. The following subsections provide more details about the stages of the ADAS prediction pipeline.

Read Frame Every frame was obtained from the ZED camera that has a 110° wide-angle lens at an aspect ratio of 16:9 and a frame resolution of 1280 × 720 captured at 30 fps. The ZED camera recorded the left and right frame as a single image; therefore a separation step was required for the left and right frames to be split into separate image arrays. The left frame array was the only frame used for object detection and tracking in our work, with the right frame being ignored, to reduce computational overheads. An ASUS laptop with an Intel i7 and a GeForce GTX 1070 was used for post-processing to run the computer vision algorithms. An NVIDIA graphics card was needed to run several algorithms that required CUDA support, to allow parallel execution with a GPU, which increases performance.

Pre-processing The second step in ADAS1 and ADAS2 was to crop the image to reduce the number of computations required. The resultant frame only included the driving and adjacent lanes as well as enough height to see the traffic lights. This frame reduction significantly reduced computation time as there were fewer pixels for each computation. In addition to reducing the frame size, several pre-processing operations were done such as converting to different color spaces, for example, grayscale. Several functions later in the ADAS prediction pipeline benefitted from this conversion to achieve a higher accuracy in the output. In ADAS2 a filter named Gaussian blur was used to prepare several frames for pixel brightness detection that would make the image more uniform.

FIGURE 7 Primary city street with traffic light and vehicle detection.

FIGURE 9 Highway with vehicle detection.

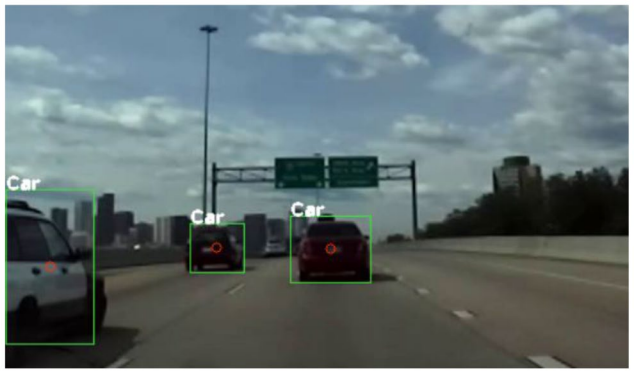

Object Detection Object detection is essential to classify features in the image, such as vehicles, signs, and traffic lights. The objective of object detection in our use case is to notify the Optimal EMS system with any possible objects that could predict or detect a possible change in vehicle speed. For example, detecting a red traffic light ahead would provide the EMS a significant advantage in predicting the potential speed reduction ahead. A Python implementation of [29] derived from the work of [30] was the CNN used for object classification in our work. An image frame is sent to the CNN layer and returns a list of objects detected with a given confidence score. Different weights and training parameters were used for the CNN models used in ADAS1 and ADAS2. One issue with the CNN classifier that we used was the inability to detect an object at a range of over 20 m. However, this was not a significant issue for our purposes of detecting vehicles, signs, and traffic lights that could directly affect the speed of the driver.

The CNN output layer indicated vehicle detection with the help of bounding boxes around those vehicles. Vehicles detected in the image were further considered only if found in the driver's lane; otherwise they were ignored. This was accomplished with a simple comparison of the centroid of the vehicle seen as a red circle in Figures 7-9. The vehicle detected was found and compared to the width of the lane. If found in the range, the object's bounding box was tracked. If the bounding box object was found to be larger in the next frame, the assumption that the vehicle was approaching can be considered to be true. If the bounding box was the same size or smaller, the vehicle was considered to remain at the same distance. Although a stereo vision camera can determine the distance of the object, the bounding box area method worked adequately for our purposes, because an exact distance is not needed to detect relative vehicle movement across frames.

Traffic light state detection was done similarly to vehicle detection with the addition of an extra processing step. A list of bounding boxes from the CNN for traffic lights was iterated and filtered based on the confidence score to select the one traffic light for object state classification that had the highest confidence. The object filtering was performed to eliminate the need to find the state of the traffic light for each sign. Stop sign and pedestrian detection were added features to ADAS1 and ADAS2, where if a confidence returned higher than 30%, the objects were identified and reported in the output file. This confidence score filtering was selected empirically, to reduce the possibility of false positives. Some segmentation techniques were also used to ensure that objects such as the sky and road were not falsely identified as people or signs.

FIGURE 8 City street with stop sign and vehicle detection.

Object Tracking For the determination of the vehicle state, the object data required a method for tracking from frame to frame. A Kalman filter was used for cases when more than one type of object was detected. The Kalman filters gave us the ability to use a linear velocity model to classify objects. From one frame to the next, an object's centroid will typically not move a significant distance, and this information can be used to filter out objects such as those that can cause false positives. In all cases, only one type of object should be detected for the tracking step in one frame because of the filtering and detection steps discussed earlier. As also discussed earlier, the best traffic light was chosen to remove the issue of multiple detections for tracking. The vehicle state classification was also the only prediction feature that required the previous information of the tracked object.

Object State Classification Traffic lights and vehicle brake lights required object state classification to determine the state of the image. Once the CNN identified these objects, additional steps were required to determine what state the traffic light indicated and if the brake lights were on. To accomplish this, the bounding box information of the objects was taken and a sub-image was created based on the size of the bounding boxes. The OpenCV function Minmax() found the location of the brightest spot in the image which would be the light's sources, which in this case is the object (traffic or brake light) to be detected. Then a circle of radius 41 pixels was used, and the average pixel color was determined after converting to a hue, saturation, value (HSV) color space. This color space conversion mitigated the effect of shadows to affect the resultant color detected. The color was then compared to find the state of the object. ADAS2 also used a Gaussian blur filter that would help identify the max pixel color more efficiently for both traffic and brake light detections.

Output Several examples of annotated output frames in Figures 7-9 illustrate the methods discussed in the previous subsection. Each figure outlines the object of interest with a bounding box and a red centroid representing the object. The information obtained for each processed frame was recorded into a CSV file. Figure 7 shows an example of the brightest point of the traffic light detected which is outlined by a blue circle. A positive detection of a stop sign can be seen in Figure 8. Figure 9 shows three detected vehicles where only the rightmost car is tracked for ADAS prediction data because it is the only vehicle in the driver's lane.

Baseline Energy Management Strategy Simulation

A 2010 Toyota Prius is selected as the vehicle model due to its commercial prevalence and because it has the highest FE in its class. The model used to represent the baseline EMS is consistent with previous research in that it is a modification of the publically available 2004 Toyota Prius in the Autonomie modeling software to represent a 2010 Toyota Prius [25]. The Autonomie modeling software has demonstrated strong correlation with real-world testing and is generally accepted as the standard among industry and research professionals [31].

The vehicle model must be validated against real-world data. Table 3 shows the simulated FE over the industry standard U.S. Environmental Protection Agency (EPA) drive cycles of the Urban Dynamometer Driving Schedule (UDDS) drive cycle, the Highway Fuel Economy Test (HWFET) drive cycle, and the US06 drive cycle. A change in battery state of charge (SOC) values must be taken into account according to the SAE J1711 industry standard [32] and the adjust FE can be reported. These numbers can then be compared to real-world measured values from Argonne National Labs [33]. When the numbers are compared, the simulation FE is within 3% of all of the physically measured FE numbers and the baseline EMS is considered validated.

TABLE 3 Simulated and measured FE for the 2010 Toyota Prius HEV model developed using Autonomie.

EPA drive cycle	Simulated FE (mpg)	Measured FE [33] (mpg)	Percentage difference (%)
UDDS	76.9	75.6	1.7
HWFET	68.8	69.9	−1.7
US06	45.9	45.3	1.3

Optimal Energy Management System Derivation

Details of an Optimal EMS derivation and implementation can be found in numerous articles [25, 34, 35]. An overall system-level viewpoint of an Optimal EMS implementation developed in previous research [27] is shown in Figure 10. This system consists of three subsystems: perception, planning, and the vehicle plant. The perception subsystem interprets the vehicle surroundings based on sensor inputs which then outputs a prediction of future vehicle velocity. The planning subsystem computes the optimal control for the provided velocity prediction. This optimal control is then actuated in the vehicle plant via the running controller which takes into account component-level limitations including SOC limits, ramp rate limits, etc.

Vehicle Operation Prediction Model In our work, ADAS data is used along with current GPS location and current vehicle velocity to predict future vehicle operation within the perception subsystem. Each of the inputs was recorded independently and did not have a direct relationship to one another. All the data was sampled at 1 Hz and was synchronized offline to match the recorded timesteps. Travel time data in the Denver area was used to provide drive cycle speeds of the entire drive cycle before the trip had begun. An artificial neural network was selected to combine the outputs

FIGURE 10 The system-level viewpoint of the Optimal EMS implementation with subsystems for perception, planning, and a vehicle plant [27].

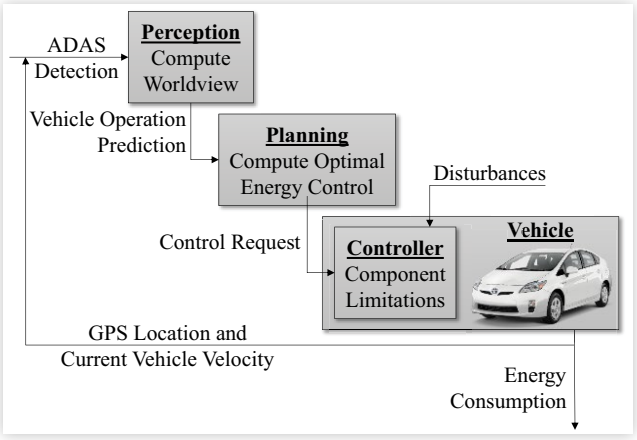

FIGURE 11 Details of the perception subsystem shown in Figure 10 that shows ADAS, GPS, and average traffic data as an input to a NARX perception model to generate a vehicle velocity prediction.

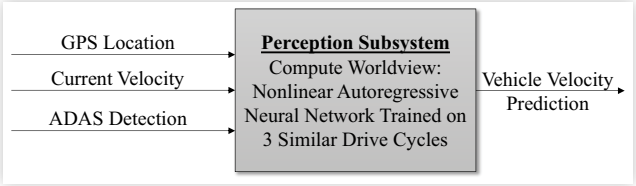

from the sensors and signals to generate a vehicle velocity prediction. We selected a nonlinear autoregressive neural network which has been demonstrated to be effective [36]. Using sensor and signal outputs to predict future velocity, a nonlinear autoregressive neural network with external inputs (NARX) is required. The future vehicle velocity values $v(t)$ are predicted from the neural network from past values of the vehicle velocity denoted as $v(t-1)$ and past values of each of the sensors and signals $x(t-1)$. The network is represented as

$$v(t) = f\left[v(t-1),\ldots v(t-d), x(t-1),\ldots(t-d)\right] \quad \text{Eq. (1)}$$

where d is the time delay. This neural network was designed in MATLAB and the NARX was trained to predict both the Denver city and highway drive cycles using three of the alternate versions of the drive cycle to be trained and the remaining drive cycle to be tested. This was done a total of four times and then was averaged. Three feedback delays, 1 hidden layer, 1 input delay, scaled conjugate gradient training, 90% data training, 2% data validation, and 8% data testing provided the best results for our chosen neural network. Figure 11 shows the function overview of the perception subsystem model.

Planning Subsystem Model

This vehicle operation prediction is then used in an optimal control algorithm that uses dynamic programming (DP) to derive the globally Optimal EMS for the given prediction. This optimal control is then issued as a control request to the vehicle's "running controller" which evaluates component limitations before actuating the vehicle plant. The object of this subsystem is to use the future vehicle operation as an input and determine the globally optimal control of the vehicle plant using DP and issues a control request to the vehicle model. The DP formulation for an HEV Optimal EMS derivation uses the battery SOC as the state variable, the engine power (P_{ICE}) as the control variable, the vehicle velocity (v) as the external input, and the total mass of fuel required (m_{fuel}) as the cost function. A detailed description of this process can be found in previous research [25]. The final form used to derive the optimal control is

$$\mathrm{SOC}(k+1) = \mathrm{SOC}(k) - C_1 + C_2\sqrt{C_3 - C_4 v(k) + C_5 v(k)^3 + C_6 \dot{v}(k) v(k) - C_7 P_{\mathrm{ICE}}} \quad \text{Eq. (2)}$$

FIGURE 12 Details of the planning subsystem shown in Figure 10 that shows generation of a globally optimal solution for the provided vehicle velocity prediction.

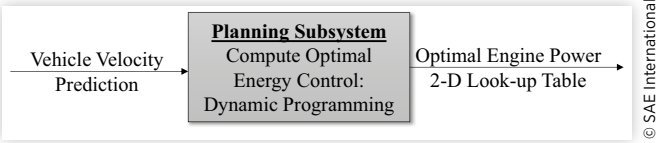

$$\mathrm{Cost} = \sum_{k=0}^{N-1} f\left(P_{\mathrm{ICE}}\right) + W\left[\mathrm{SOC}_f - \mathrm{SOC}(N)\right]^2 \quad \text{Eq. (3)}$$

$$40\% \le \mathrm{SOC}(k) \le 80\% \quad (k = 0,\ldots,N) \quad \text{Eq. (4)}$$

$$0\ \mathrm{kW} \le P_{\mathrm{ICE}}(k) \le 73\ \mathrm{kW} \quad (k = 0,\ldots,N-1) \quad \text{Eq. (5)}$$

$$C_8\left[f\left(P_{\mathrm{ICE}}\right)\right] + C_9 v(k) \le C_{10} \quad \text{Eq. (6)}$$

where C_{1-10} are constants, k is an arbitrary timestep, N is the final timestep, and W is a penalty weighting factor. SOC_f is the desired final SOC of the battery which is set to 50% to allow a charge-sustaining behavior. Therefore, the process of perception, planning, and vehicle actuation uses second-by-second feedback with the Optimal EMS computed for 15-second predictions which has been shown in previous research to be an effective prediction window for achieving FE improvements [26]. Plots of the output of this particular algorithm are shown in another research paper from the authors [34]. Figure 12 shows the overview of the planning subsystem model.

Vehicle Subsystem Model

The input to the vehicle model is the Optimal EMS control request and disturbances attributed to misprediction. The vehicle model used is a 2010 Toyota Prius Autonomie model that we created (by extending the baseline 2004 Toyota Prius Autonomie model) and verified. This model includes a running controller, which enforces individual component operation limitations. The recorded output of this model can be any variable inherent in the Autonomie software. Of particular interest is the fuel consumption, achieved engine power, and battery SOC. These results can then be compared to the same outputs from baseline EMS simulation.

An overall conceptual diagram of the vehicle subsystem model is shown in Figure 13. The main output of the vehicle

FIGURE 13 Details of the vehicle plant subsystem shown in Figure 10 that received the modified control request and implements it with the vehicle running control for FE measurements.

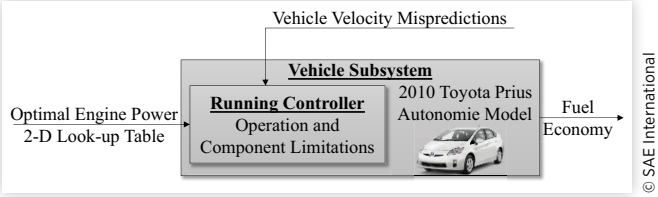

subsystem is achieved charge-adjusted FE which can be calculated according to the current SAE standard [35]. Because ADAS detection provides limited (line of sight) future drive cycle predictions, it is not possible to predict speeds along the entire drive cycle from ADAS data points at time zero.

Results

ADAS Output Comparison

Figures 14-16 show the comparison of each frame input of ADAS1 and ADAS2 to ground truth. As each of the two drive cycles was driven four times, results for a total of eight videos are shown with a comparison of ground truth to the Optimal EMS ADAS prediction with ADAS1 and ADAS2. From Figure 14 we can see the stop sign comparison to the ground truth was around 98% for ADAS1 and 99% for ADAS2. This difference was most likely due to the different weights and parameters files used during detection. The stop sign accuracy rate was found to be very high because only one stop sign was encountered in both drive cycles. The CNN used gave very low false positive and could detect the stop sign in most videos; however, it failed to detect the stop sign at large distances in contrast to the ground truth data. This drive cycle only contained one stop sign, giving very limited useful data on this metric for object detection for Optimal EMS. We speculate that with the addition of more stop signs, the Optimal EMS may be able to predict the vehicle speed with greater accuracy and lead to better FE increase. Further studies on how stop signs affect this data will be incorporated in future tests.

For the vehicle in-front state, we can see from Figure 15 that the average accuracy was around 60% for ADAS1 and 70% for ADAS2. The accuracy improved from ADAS1 to ADAS2 due to the different weight and configuration files used for detection. This accuracy was also improved in ADAS2 due to the slight change in the tracking algorithm that classified the vehicle state. A small buffer was added to add more "same" cases if a vehicle was detected recently. However, the CNN in both ADAS1 and ADAS2 failed to identify objects at distances farther than 20 m. The ground truth data labeled by hand annotated vehicles at a much more significant range.

For traffic lights, the average accuracy for the odd videos (highway drive cycles) was around 70%, while the average accuracy for the even videos (city drive cycles) was 40%, as shown in Figure 16. Counting the total traffic lights, it was found that 59 traffic lights were encountered in the city drive cycle and 16 in the highway cycles, which means that approximately 23 traffic lights were detected in the city drive cycle

FIGURE 14 ADAS percent accurate to ground truth—stop sign state.

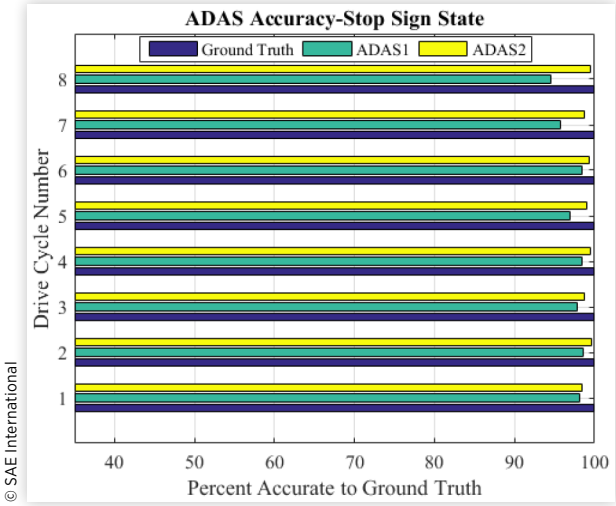

FIGURE 15 ADAS percent accurate to ground truth—vehicle in-front state.

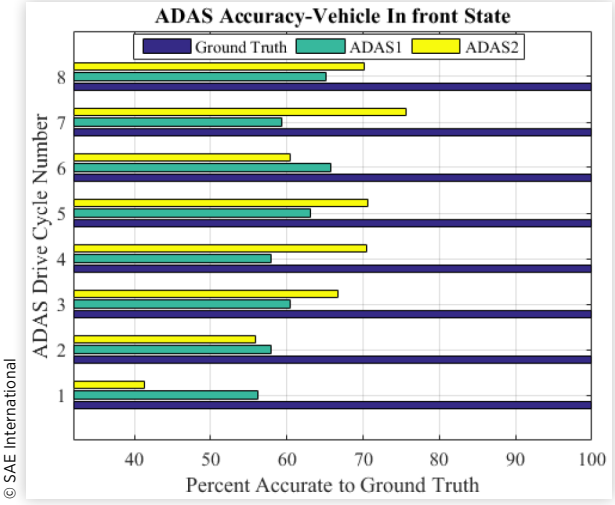

FIGURE 16 ADAS percent accurate to ground truth—traffic light state.

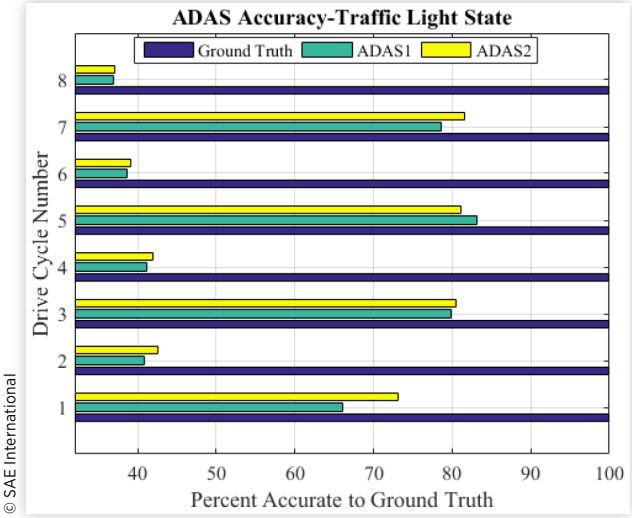

and 11 in the highway. The inaccuracies were due to the changing ambient lighting and diverse positioning of the traffic light. Many frames of the traffic light were blocked by cars and were detected for ground truth at a much higher distance (similar to the issues faced with the vehicle in-front state). Most traffic lights were also of smaller size than vehicles and only provided positive readings during object detection when the vehicle was within 5 m of the light. The accuracy of detection of stop light colors was also challenging to get correct. Relying on the average color of the pixels was found to be an ineffective predictor for these lights.

Fuel Economy Improvements with ADAS

Insights into the FE improvements that are possible when ADAS detection data is combined with an Optimal EMS can be obtained using a difference in battery charge-adjusted FE [32] from the baseline EMS and the Optimal EMS calculated as

$$\text{Percent improvement} = \frac{FE_{Optimal} - FE_{Baseline}}{FE_{Baseline}}$$

The ADAS detection Optimal EMS FE improvements must also be put in context with the globally Optimal EMS FE improvements. The globally Optimal EMS FE improvement is possible when the entire drive cycle is predicted 100% accurately from time zero. This serves as an important reference point to understand the scope of the FE increase that can be realized through ADAS detection. We also define a new metric called "prediction window optimal," which is the optimal prediction of a 15-second window used for ADAS1 and ADAS2.

Figure 17 shows the comparison for city-focused drive cycle between the globally Optimal EMS strategy, the two ADAS strategies (ADAS1, ADAS2), and the ground truth ADAS strategy. All results are presented relative to the baseline control strategy for the 2010 Toyota Prius. The globally Optimal EMS FE improvement is 19.6%, which represents an upper bound on the improvements in FE that can be achieved. The prediction window optimal FE improvement is 11.9%. With ground truth ADAS detection, approximately half of this amount is realized at 6.1%, which is a very promising result. Using the actual algorithms developed and implemented, a 4.4% improvement was realized with ADAS1, and a 5.3% improvement was realized with ADAS2. The difference between the ground truth ADAS and results from the actual ADAS deployments (ADAS1, ADAS2) was due to the inaccuracies and limitations with the real-time computer vision algorithms. In particular, the failure to detect an object at great distances reduced the accuracy in many cases. Another source of error was with the traffic light state detection, as discussed earlier. There were also several difficulties in producing accurate results in time to make an impact on FE. ADAS2 give a slightly higher percentage increase in FE than ADAS1. As discussed earlier, this was primarily due to the different set of weighting and training parameters and the addition of vehicle brake light data.

Figure 18 shows the FE comparison for highway-focused drive cycle between the globally Optimal EMS strategy, the two ADAS strategies (ADAS1, ADAS2), and the ground truth ADAS strategy. All results are relative to the baseline control strategy for the 2010 Toyota Prius. The globally Optimal EMS improvement is 10.9%, which is lower than the FE available from the city-focused driving cycle due to the lower frequency of stops and starts during highway driving. The prediction window optimal FE improvement was found to be 8.3%. However, the ground truth ADAS detection realized only 1.94%. Using the algorithms developed and implemented, a 1.9% FE improvement was realized with ADAS1, and a 1.1% FE improvement was realized with ADAS2. As discussed in earlier sections, the decrease in FE in comparison to city

FIGURE 17 City-focused drive cycle comparison of FE for 2010 Toyota Prius with various strategies: Optimal EMS improvement in FE realized through 100% accurate detection of the entire drive cycle (globally Optimal FE increase), 100% accurate ADAS detection (ground truth ADAS FE increase), and the algorithms that compose ADAS1 and ADAS2. All results are relative to the baseline control strategy used in the 2010 Toyota Prius.

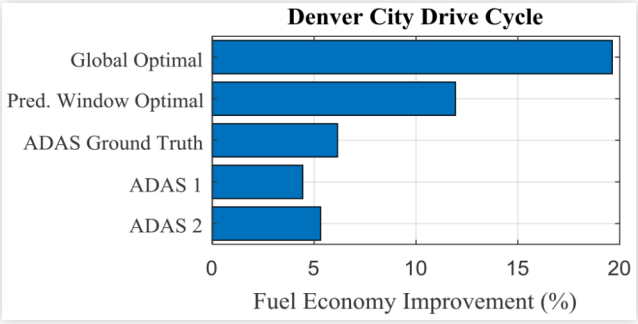

FIGURE 18 Highway-focused drive cycle comparison of FE for 2010 Toyota Prius with various strategies: Optimal EMS improvement in FE realized through 100% accurate detection of the entire drive cycle (globally Optimal FE increase), 100% accurate ADAS detection (ground truth ADAS FE increase), and the algorithms that compose ADAS1 and ADAS2. All results are relative to the baseline control strategy used in the 2010 Toyota Prius.

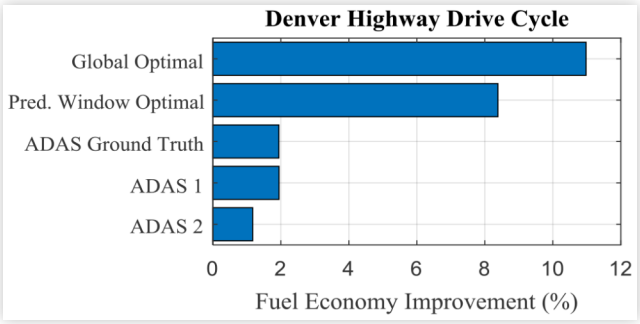

driving is in a large part due to the issue with the range of detection and the less frequent stops. These results illustrate that the highway-focused drive cycle shows significantly lower FE increase relative to the city-focused driving cycle, for all of the tested ADAS algorithms.

Conclusions and Future Work

In this study, a novel prediction approach for use in Optimal EMS was developed using ADAS technology. A methodology was developed to determine what information ADAS could provide to improve FE. Two ADAS strategies (ADAS1 and ADAS2) using computer vision were developed and compared and showed notable improvements in FE.

Overall, these promising results suggest that modern commercially available ADAS technology could be repurposed to implement an Optimal EMS in modern vehicles. As new sensing capabilities become commercially available as part of ADAS systems, the FE improvements possible through an Optimal EMS may start to approach the globally Optimal EMS results. We are currently expanding our work to utilize a range of V2X inputs into the prediction model. Our next study will explore the potential FE improvements that are realizable with these richer data sets.

Contact Information

Jordan Tunnell
Colorado State University, Fort Collins, CO 80523 USA
Jordantunnell@gmail.com

Acknowledgments

This article is an updated and significantly revised version of a presentation at WCX18, Detroit, MI, April 10-12, 2018 [37].

Definitions/Abbreviations

ADAS - Advanced driver-assistance system

FE - Fuel economy

EMS - Energy management strategy

HEV - Hybrid electric vehicle

Ground Truth - A set of measurements that are provided by direct (human) observation

References

1. International Energy Agency, "Key World Energy Statistics 2016," International Energy Agency, 2015.
2. Energy Information Administration, "Annual Energy Outlook 2017," 2017.
3. Lukic, S.M. and Emadi, A., "Effects of Drivetrain Hybridization on Fuel Economy and Dynamic Performance of Parallel Hybrid Electric Vehicles," *IEEE Trans. Veh. Technol.* 53:385-389, 2004, doi:10.1109/TVT.2004.823525.
4. Lin, C.-C., Kang, J.-M., Grizzle, J.W., and Peng, H., "Energy Management Strategy for a Parallel Hybrid Electric Truck," *Proceedings of the 2001 American Control Conference*, Cat. No. 01CH37148, Vol. 4, 2878-2883. 2001, ieeexplore.ieee.org.
5. Kim, N., Cha, S., and Peng, H., "Optimal Control of Hybrid Electric Vehicles Based on Pontryagin's Minimum Principle," *IEEE Trans. Control Syst. Technol.* 19:1279-1287, 2011, doi:10.1109/TCST.2010.2061232.
6. Michel, P., Karbowski, D., and Rousseau, A., "Impact of Connectivity and Automation on Vehicle Energy Use," SAE Technical Paper 2016-01-0152, 2016, doi:10.4271/2016-01-0152.
7. Son, J., Park, M., and Kim, B., "Effect of Advanced Driver Assistance Systems on Driving Style and Fuel Economy," *Age* 27:60-69.
8. Rajamani, R., *Vehicle Dynamics and Control* (Springer Science & Business Media, 2011).
9. Bender, F.A., Kaszynski, M., and Sawodny, O., "Drive Cycle Prediction and Energy Management Optimization for Hybrid Hydraulic Vehicles," *IEEE Trans. Veh. Technol.* 62:3581-3592, 2013.
10. van Keulen, T., van Mullem, D., de Jager, B., Kessels, J.T.B.A. et al., "Design, Implementation, and Experimental Validation of Optimal Power Split Control for Hybrid Electric Trucks," *Control Eng. Pract.* 20(5):547-558, 2012.
11. Pagliara, E., Parlangeli, G., Donateo, T., and Adamo, F., "Real Time Implementation of an Optimal Power Management Strategy for a Plug-In Hybrid Electric Vehicle," *52nd IEEE Conference on Decision and Control*, 2013, 2214-2219, ieeexplore.ieee.org.
12. Wang, L., Zhang, Y., Yin, C., Zhang, H. et al., "Hardware-in-the-Loop Simulation for the Design and Verification of the Control System of a Series-Parallel Hybrid Electric City-Bus," *Simulation Modelling Practice and Theory* 25(6):148-162, 2012.
13. Opila, D.F., Wang, X., McGee, R., and Grizzle, J.W., "Real-Time Implementation and Hardware Testing of a Hybrid Vehicle Energy Management Controller Based on Stochastic Dynamic Programming," *J. Dyn. Syst. Meas. Control* 135:021002, 2013.
14. Rizzoni, G. and Onori, S., "Energy Management of Hybrid Electric Vehicles: 15 Years of Development at the Ohio State University," *Oil & Gas Science and Technology - Revue d'IFP Energies Nouvelles* 70:41-54, 2015.
15. Asher, Z.D., Trinko, D.A., and Bradley, T.H., "Increasing the Fuel Economy of Connected and Autonomous Lithium-Ion Electrified Vehicles," in *Behaviour of Lithium-Ion Batteries in Electric Vehicles: Battery Health, Performance, Safety, and Cost*, eds. G. Pistoia and B. Liaw (Cham, Springer International Publishing, 2018), 129-51.

16. World Health Organization (WHO), "Global Status Report on Road Safety 2015," http://www.who.int/violence_injury_prevention/road_safety_status/2015/en/.
17. Association for Safe International Road Travel (ASIRT), "Annual Global Road Crash Statistics," http://asirt.org/initiatives/informing-road-users/road-safety-facts/road-crash-statistics.
18. Stephanie, A., Yves, P., Ulrich, S., Felix, F. et al., "Prospective Effectiveness Assessment of ADAS and Active Safety Systems via Virtual Simulation: A Review of the Current Practices," 2017, Trid.trb.org, https://trid.trb.org/view.aspx?id=1481018.
19. Knauss, A., Berger, C., and Eriksson, H., "Towards State-of-the-Art and Future Trends in Testing of Active Safety Systems," *Proceedings of the 2nd International Workshop on Software Engineering for Smart Cyber-Physical Systems (SEsCPS '16)* (New York: ACM, 2016), 36-42.
20. Nieto, M., Vélez, G., Otaegui, O., Gaines, S. et al., "Optimising Computer Vision Based ADAS: Vehicle Detection Case Study," *IET Intelligent Transport Systems IET Digital Library* 10(3):157-164, 2016.
21. Suriya, N.L. and Viswanath, P.,."Improved Ground Plane Detection in Real Time Systems Using Homography," *2014 IEEE International Conference on Consumer Electronics (ICCE)*, 2014, 199-200.
22. Zolock, J., Senatore, C., Yee, R., Larson, R. et al., "The Use of Stationary Object Radar Sensor Data from Advanced Driver Assistance Systems (ADAS) in Accident Reconstruction," 2016, http://papers.sae.org/2016-01-1465/.
23. Dadras, S., "Path Tracking Using Fractional Order Extremum Seeking Controller for Autonomous Ground Vehicle," SAE Technical Paper 2017-01-0094, 2017, doi:10.4271/2017-01-0094.
24. Kukkala, V.K., Tunnell, J., Pasricha, S., and Bradley, T., "Advanced Driver-Assistance Systems: A Path toward Autonomous Vehicles," *IEEE Consumer Electronics Magazine* 7(5):18-25, 2018.
25. Asher, Z.D., Baker, D.A., and Bradley, T.H., "Prediction Error Applied to Hybrid Electric Vehicle Optimal Fuel Economy," *IEEE Trans. Control Syst. Technol.* 1-14, 2017, doi:10.1109/TCST.2017.2747502.
26. Baker, D., Asher, Z., and Bradley, T., "Investigation of Vehicle Speed Prediction from Neural Network Fit of Real World Driving Data for Improved Engine On/Off Control of the EcoCAR3 Hybrid Camaro," SAE Technical Paper 2017-01-1262, 2017, doi:10.4271/2017-01-1262.
27. Asher, Z., Wifvat, V., Navarro, A., Samuelsen, S. et al., "The Importance of HEV Fuel Economy and Two Research Gaps Preventing Real World Implementation of Optimal Energy Management," SAE Technical Paper 2017-26-0106, 2017, doi:10.4271/2017-26-0106.
28. Zed Stereo Camera, https://www.stereolabs.com/.
29. Darknet YOLO Python, https://github.com/thtrieu/darkflow.
30. Redmon, J. Farhadi, A. and, "YOLO9000: Better, Faster, Stronger," arXiv preprint arXiv: 1612.08242, 2016.
31. Kim, N., Rousseau, A., and Rask, E., "Autonomie Model Validation with Test Data for 2010 Toyota Prius," SAE Technical Paper 2012-01-1040, 2012, doi:10.4271/2012-01-1040.
32. SAE International, "Recommended Practice for Measuring the Exhaust Emissions and Fuel Economy of Hybrid-Electric Vehicles," 2002.
33. Argonne National Lab, "Downloadable Dynamometer Database," 2015, https://www.anl.gov/energy-systems/group/downloadable-dynamometer-database/hybrid-electric-vehicles/2010-toyota-prius
34. Asher, Z.D., Tunnell, J.A., Baker, D.A., Fitzgerald, R.J. et al., "Enabling Prediction for Optimal Fuel Economy Vehicle Control," SAE Technical Paper 2018-01-1015, 2018, doi:10.4271/2018-01-1015.
35. Zhang, P., Yan, F., and Du, C., "A Comprehensive Analysis of Energy Management Strategies for Hybrid Electric Vehicles Based on Bibliometrics," *Renewable Sustainable Energy Rev* 48:88-104, 2015.
36. Demuth, H.B., Beale, M.H., De Jess, O., and Hagan, M.T., *Neural Network Design* (USA: Martin Hagan, 2014).
37. Tunnell, J.A.,Asher, Z.D., Pasricha, S., and Bradley, T.H., "Towards Improving Vehicle Fuel Economy with ADAS," SAE Technical Paper 2018-01-0593, 2018, doi:10.4271/2018-01-0593.